Electronic structure and morphology of MgO submonolayers at the Ag(001) surface: An *ab initio* model study

Anna M. Ferrari,* Silvia Casassa, and Cesare Pisani
Dipartimento di Chimica IFM, Università di Torino and Centre of Excellence NIS (Nanostructured Interfaces and Surfaces), Via Giuria 5, I-10125 Torino, Italy
(Received 20 July 2004; published 7 April 2005)

Submonolayer structures of MgO epitaxially deposited on Ag(001) have been simulated theoretically in order to gain information on the mode of growth. The model adopted consists in a thin silver slab covered on both sides by MgO "polymers" (narrow ribbons monoatomic in height) sufficiently distant to prevent interactions among them. An *ab initio* DFT periodic technique has been adopted, whose adequacy has previously been checked for the case of perfect complete MgO/Ag overlayers. Two orientations of the polymers have been considered, corresponding to two modes of growth experimentally observed: a nonpolar (*NP*) and a polar (*P*) one, the latter being limited at the two borders by rows of bicoordinated O and Mg ions. We have considered both the case where the polymers sit (are "supported") on the flat metal surface, and where they are "embedded" in grooves at the surface. The results of the simulations (equilibrium geometries, electronic structure and energy data) can be summarized as follows: (i) Interaction with the metal substrate enormously contributes to reducing the instability of the polar border; nevertheless, both for islands supported or embedded at the silver surface, the role of the metal is not sufficient to stabilize the *P*- with respect to the *NP* orientation. (ii) Steps or vacancy depressions at Ag(001) with edges oriented along the silver ⟨110⟩ symmetry direction are considerably favored (by almost 25% per unit length) over the ⟨100⟩ oriented edges in agreement with observations; the preexistence of the former type of steps may favor kinetically the nucleation of *P*-oriented islands leaning against them. (iii) The formation of islands embedded in the metal is in all cases thermodynamically favored with respect to supported ones; this means that, in favorable conditions, the growing oxide film might displace silver atoms and penetrate to some extent in the metal. (iv) The electronic and electrostatic features at polar borders suggest that they could be characterized by very high chemical activity.

DOI: 10.1103/PhysRevB.71.155404 PACS number(s): 68.55.−a, 71.15.Mb, 68.35.Ct

I. INTRODUCTION

Thin epitaxial oxide films on metal substrates [1–10 monolayers (ML)] have received considerable attention in recent years, because of their prospective technological importance (for instance, in the fields of electronics and catalysis) and for their relevance in the understanding of the metal-oxide interface.[1–3] In particular, the MgO/Ag(001) system has been the object of a number of studies[4–13] due to the very simple structure of the oxide and the moderate lattice mismatch between MgO (lattice constant 4.21 Å) and the Ag substrate (lattice constant 4.09 Å). Combined experimental techniques (STM, EXAFS, PDMEE) and computational approaches have been employed to investigate the electronic structure and morphology of this metal-oxide interface.[14,15] Accurate estimates of relevant geometrical parameters obtained by experimental techniques and *ab initio* calculations have resulted in excellent agreement.[14–17] With reference to an idealized model of a perfect interface, both PDMEE and theory indicate that the oxide grows forming epilayers with oxygen on-top of silver atoms; the interface distance [$d_{\mathrm{Ag\text{-}MgO}}=2.51$ and 2.55 Å from EXAFS (Ref. 18) and *ab initio methods*,[14] respectively] shows a tetragonal strain due to the constraints of perfect epitaxy. With respect to the unsupported film, the computed electronic structure of the oxide reveals only moderate variations confined in a strict vicinity of the interface. The latter findings seem in contrast, however, with other experimental observations. A considerable enhancement of the chemical reactivity of the supported film has been in fact observed,[19,20] together with other evidence of a modified electronic structure, such as the shift of the oxygen core levels or the appearance of electron states close to the Fermi level.[9] Since the perfect epilayer cannot account for these observations,[14] the reason for such behavior could tentatively be attributed to some residual defectivity of the thin film. An accurate analysis of the early stages of the film growth, namely at a nominal deposition of less than 1 ML, can provide new insight in this respect: the intrinsic defectivity of the submonolayer could both give rise to peculiar electron properties and reactivity and drive the morphology and amount of structural defects in thicker films.

STM experiments have given very useful indications on the film morphology.[12,13] Before the MgO deposition, the Ag(001) surface exhibits large terraces separated by monoatomic steps with the edge oriented along the Ag ⟨100⟩ symmetry direction and mean separation of more than 100 nm. Upon a nominal deposition of 0.25 ML of MgO, STM images reveal a complex change in the morphology of the metal substrate: a limited number of flat extended islands are detected on the terraces, both of a "protruding" and of a "vacancy" type, while a large number of small islands appear on the substrate surface and on top of the large islands.[13] The small islands are composed of MgO, while the larger structures are identified as Ag islands that have formed on the original metal surface. The MgO structures are mainly monoatomic in height but a limited amount of bilayers and

trilayers has been detected at 0.75 ML MgO deposition and becomes significant at 1 ML deposition. At 1 ML nominal deposition the substrate fractional coverage is about 85% with the formation of flat square MgO domains of about 10 nm in width with edges mainly oriented along the oxide ⟨110⟩ symmetry direction. For definiteness, and to avoid confusion, this will be called the *P* orientation, *P* standing for polar (see below). A relevant number of three-dimensional (3D) pyramidal MgO islands is present, their edges being again *P* oriented.[13] The *P* orientation is also the prevailing one in submonolayer islands of NiO/Ag(001).[21] In the MgO case, the *P* or *NP* orientation seems to be related to the specific conditions in which the experiments are run: other laboratories report STM images which show MgO islands *mainly NP* oriented, that is, along the ⟨100⟩ oxide symmetry direction[12] (*NP* standing for nonpolar). In any event, the possible formation of *P*-oriented MgO islands is surprising. Bicoordinated ions of just one species would be found at their borders (O on one side, Mg on the opposite), so they would be characterized by a high transverse dipolar moment which is expected to destabilize the structure. This problem has some analogy with that of polar surfaces, which are well known to undergo reconstruction in order to reduce their electrostatic instability.[22,23] On the other hand, the presence of the metal substrate could play an important role in favoring such an unexpected orientation. Low coordination border ions could give rise to special electronic features and to enhanced chemical reactivity.

These questions have been addressed in this work. Quantum chemical calculations and periodic models have been employed to analyze the early stages of the growth of the MgO monolayer in order to better understand the morphology and electronic structure of the growing film, and the role—if any—of the metal substrate in driving this process. A preliminary and partial account of the present results has been provided in a parallel paper, along with the critical presentation of the experimental STM evidence.[24]

II. METHOD AND MODELS

MgO "polymers" are employed here as a crude model of MgO islands growing at the silver surface. As shown in Fig. 1, they are arranged to form ordered arrays at the Ag slab, which allows us to adopt a two-dimensional supercell (SC) technique. Polar and nonpolar borders have been modeled by polymers *P* or *NP* oriented, respectively. The thickness of the polymers has been limited to a single layer, while two possibilities were considered for their width, resulting in *P*1, *P*2, *NP*1, *NP*2 structures. The polymers are either epitaxially adsorbed above the Ag surface ("supported" or *S* models) or "embedded" in grooves at the slab surface (*E* models). The SCs adopted are shown in Fig. 1; in all cases, the same pattern is assumed to exist on both sides of the slab. The selected elementary cell, comprising four Ag atoms per layer inside the slab, despite its moderate size, has been tested to be large enough to avoid significant interaction between adjacent polymers. The interaction energy between unsupported polymers placed at the same distance as when supported or embedded is actually negligible for nonpolar

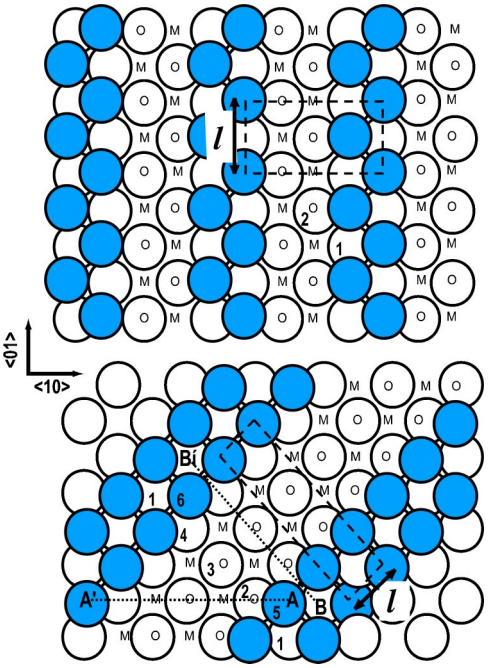

FIG. 1. (Color online) Schematic top view of the structures considered. The large white circles are Ag atoms in the surface plane (Π) of the three-layer slab; the grey circles are Ag atoms atop Π, which are present only in the case of the "embedded" E models for the nonpolar (*NP*: top graph) and polar (*P*: bottom graph) supported polymers. The *P*2 and *NP*2 polymers are shown in the graphs, with the magnesium (M) and oxygen (O) ions at their unrelaxed positions. The unit supercell (SC) is represented by the dashed rectangle; *l* is the length per unit SC of the polymer border. In the bottom plot, $A---A'$ and $B---B'$ are the intersection with the surface of the maps of Fig. 3; numbers 1 to 6 identify symmetry independent Ag atoms in the Π plane and in the rows above it. For the one-row polymers the SC is the same as in the case depicted here but the polymer has half that width. In the *E*-*P*1 case, two possibilities are treated according to whether Mg or O ions are close to the border of the groove (*E*-$P1_{Mg}$ or *E*-$P1_{O}$, respectively). The crystallographic directions are indicated in the scheme at the center of the graph.

systems and less than 0.2 eV for the polar case. Because of the stabilizing effect of the metal substrate, these small interactions are expected to become even less relevant when the polymers are supported. For the *S* models, the metal support is simulated by a three-layer slab exposing the (001) face, corresponding to two (*S*-*P*1, *S*-*NP*1) or four (*S*-*P*2, *S*-*NP*2) MgO units and 12 Ag atoms per SC. In the *E* models, there are two additional Ag atoms per SC in each of the two surface layers, which makes a total of 16 Ag atoms per SC. The central slab layer is a reflection plane in all cases.

Calculations have been performed using the CRYSTAL code[25] in the frame of density functional theory (DFT). The PWGGA (Ref. 26) exchange-correlation functional has been used, which was found to satisfactorily reproduce the bulk properties of both the metal and the oxide. The basis set adopted consists of all-electron 8-61G and 8-51G functions for Mg and O, respectively; for silver, a small-core pseudopotential was used, while for the outer electrons a variationally optimized set was adopted comprising 4,4,2 contracted

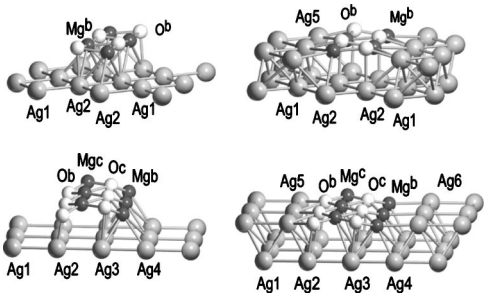

FIG. 2. Prospective views of *P*2 and *NP*2 MgO polymers supported and embedded at the Ag(001) surface in their equilibrium configuration. White spheres, O; gray spheres, Ag; black spheres, Mg.

Gaussian type functions (GTF) of type s,p, and d, respectively. Other details are reported in previous work.[14,16] Geometry optimizations have been carried out using the procedure recently implemented in CRYSTAL. However, at present, only numerical gradients are available for conductors: this restriction has placed serious limitations to the number of degrees of freedom that are allowed to relax, and only the coordinates of O and Mg ions have been optimized. Energy data reported in this work are not corrected for the basis set superposition error.[27] However, this error has been estimated to be of the same entity (0.3–0.4 eV per MgO unit) for all systems and therefore should not affect energy differences and comparative stabilities. Kohn-Sham eigenvalues corresponding to oxygen 1*s* core levels have been considered in order to gain information on the electronic structure at the interface. Their use as a measure of the core level binding energy is not fully justified in DFT, but is validated by experience.[28]

III. RESULTS AND DISCUSSION

A. Characterization of supported and embedded polymers

We shall first discuss the results for the supported and embedded *P*2 and *NP*2 structures. Figures 2 and 3 provide a schematic representation of their equilibrium configuration, while Table I collects pertinent geometrical and electron structure data. In the following discussion, we take as a reference the perfect epitaxial MgO monolayer on (001) silver (briefly, 1 ML); all data for this structure are from Table 2 of Ref. 14 (column PWGGA, Rumpling).

*S-NP*2 strongly resembles 1 ML; O ions are almost perfectly on top of silver atoms, while Mg ions undergo considerable rumpling (0.21 Å; 0.16 in 1ML) in order to reduce the surface dipolar moment. In fact, the presence of the overlayer causes a moderate polarization of the surface: owing to a Mulliken analysis, about 0.17 electrons flow from the polymer to the metal per each surface silver atom (0.20 in 1 ML). Due to the reduced coordination in the polymer, O is significantly less ionic than in the complete overlayer [q(O) $=-1.50$ a.u., -1.77 in 1 ML]; as a consequence, the interaction with the metal substrate suffers less from Pauli repulsion between metal atoms and ad-anions, and the oxide can approach closer the metal surface [z(O)$=2.40$ Å; 2.55 in 1 ML]. Correspondingly, the adhesion energy between the metal and the oxide polymer is about twice as high (1.31 eV/MgO; 0.65 in 1 ML). The same polymer embedded in a silver groove (model *E-NP*2 of Figs. 1 and 2) does not present important differences in the structural parameters. Note only that the oxygen ions are significantly farther from the Ag atoms beneath [z(O)$=2.62$ Å] probably due to the interaction with the silver atoms at their same level. The overall effect is an increased adhesion energy (1.74 eV/MgO).

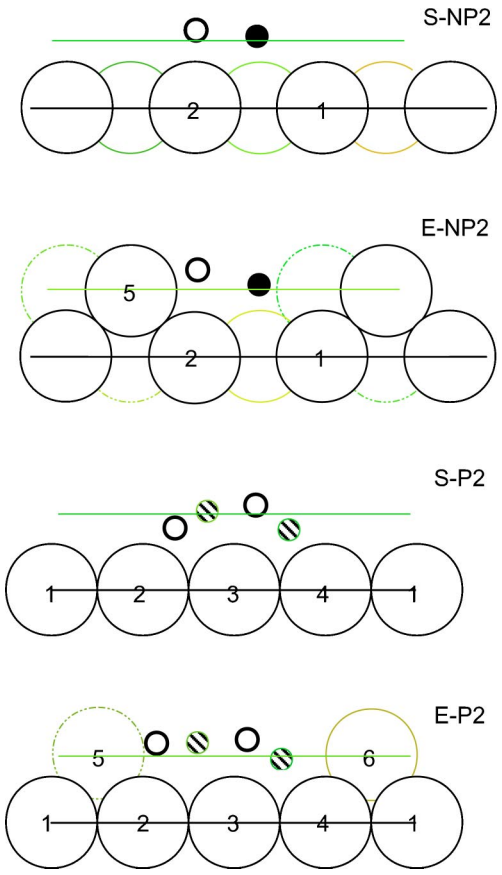

FIG. 3. Vertical view of the equilibrium configurations of O (white) and Mg (black) ions for the different cases, as indicated. The sections of polar polymers are along the $B—B'$ line of Fig. 1, and contain the surface Ag atoms (1 to 4) and the O ions; the Mg ions behind (with white stripes), and atoms Ag_5 and Ag_6 (dashed contours) in the case of *E-P*2, are also shown. The dashed horizontal line is 2.05 Å above the surface, corresponding to the interlayer distance in silver.

We turn now to discussing the results for the polar polymers (models *S-P*2 and *E-P*2). In analogy with polar surfaces on a metal support, where the high electron mobility in the metal can favor the charge reorganization of the adlayer,[29] we can expect the same mechanism to act here to reduce the electrostatic instability of the polar border. Charge redistribution is made evident by difference density maps, such as reported in Fig. 4 concerning *E-P*2. They are obtained by plotting the difference between the electron density of the interacting system in its equilibrium configuration, and the superposition of the densities of the two moieties (*P*2 polymer and grooved silver slab) calculated independently

TABLE I. Main features of the model systems sketched in Fig. 1. z (the height above the slab surface), Δx (ion displacement parallel to the surface and perpendicular to the polymer, in the O $\rightarrow$Mg direction), d (selected O-Ag distances) in Å; q (Mulliken net charge) in a.u.; BE(O_{ls}) (oxygen core level binding energy), and $\delta\varepsilon_F$ (shift of the Fermi level with respect to the isolated metal slab) in eV; ΔE_{ad} (adhesion energy) and ΔE_{stab} (stabilization energy) in eV per MgO unit. For the *P*2 polymers, border and nonborder ions are identified by subscripts *b* and *c*, respectively. The numbering of silver atoms is as in Fig. 1.

	*S-NP*2	*S-P*2	*E-NP*2	*E-P*2
$z;\Delta x(O_b)$	2.385;0.037	1.890;0.96	2.619;0.079	2.401;0.43
$z;\Delta x(O_c)$		2.621;0.69		2.527;0.38
$z;\Delta x(Mg_c)$		2.423;0.57		2.462;0.25
$z;\Delta x(Mg_b)$	2.174;0.0	1.852;0.26	2.148;0.0	1.954;0.12
$d(O_b\text{-}Ag_5)$			2.207	2.402
$d(O_b\text{-}Ag_2)$	2.405	2.118	2.621	2.439
$q(O_b)$	−1.50	−1.38	−1.46	−1.37
$q(O_c)$		−1.66		−1.63
$q(Mg_b)$	1.85	1.85	1.85	1.87
$q(Mg_c)$		1.83		1.83
$q(Ag_1)$	−0.22	−0.04	−0.12	0.00
$q(Ag_2)$	−0.17	0.30	−0.16	0.06
$q(Ag_3)$	−0.17	−0.32	−0.16	−0.35
$q(Ag_4)$	−0.22	−0.65	−0.12	−0.40
$q(Ag_5)$			−0.13	0.28
$q(Ag_6)$			−0.13	−0.32
$\delta\varepsilon_F$	1.20	1.32	1.28	0.62
$BE(O_{b,ls})$	507.7	506.9	508.6	508.0
$BE(O_{c,ls})$		508.3		509.1
ΔE_{ad}[a]	−1.31	−6.51	−1.74	−7.07
ΔE_{stab}[b]	1.24	1.65	0.81	1.09

[a]Computed with respect the isolated moieties: $\Delta E_{ad} = (E(\text{polymer})/[\text{Ag}(001)] - \{E[\text{Ag}(001)] + E(\text{polymer})\})/n$. All energies are referred to the same SC, and n is the number of MgO units in the SC.

[b]Computed with respect the supported MgO monolayer: $\Delta E_{stab} = \{E(\text{polymer})/[\text{Ag}(001)] - nE^0\}/n$, where E^0 is the energy (per MgO unit) of the supported monolayer and n is the number of MgO units in the SC.

but at the same geometry. The depletion of an electron charge at the negative border of the polymer is evident from these maps and from the Mulliken population data of Table I, and concerns both the border oxygen [$q(O^b) = -1.37$ a.u.] and the silver atoms facing it [$q(Ag^5) = +0.28$ a.u.]. Electrons flow to a tubular region of almost uniform negative charge around the positive border, both in front of the Mg ions [$q(Ag^6) = -0.32$ a.u.] and beneath [$q(Ag^3) = -0.35$ a.u.; $q(Ag^4) = -0.40$ a.u.]. Since these important charge displacements take place approximately parallel to the surface, the increase in the value of the Fermi level is not as large as for the *S* cases. The stabilization provided by this kind of image charge is enormous, as indicated by the adhesion energies ($\Delta E_{ad} = -6.51$ and -7.07 eV/MgO for the *S-P*2 and *E-P*2 systems, respectively); see Table I. The difference in stability between the polar and nonpolar structures is remarkably reduced, from 5.61 eV/MgO for the unsupported polymers to 0.41 and 0.28 eV/MgO for supported and embedded polymers, respectively. At variance with *NP* polymers, the equilibrium geometry of the polar structures is very different from that of the ideal monolayer,[14] as is apparent from Figs. 2 and 3 and Table I. The effect is more spectacular in the *S-P*2 case. Due to the attraction between the two borders, the film is squeezed by 0.70 Å, and is tilted towards its positive end. Mg_b ions approach as much as possible the closest surface atom (Ag_4), without getting too far from the nearby oxygens: their distance from Ag_4 decreases from 2.98 Å, as in *S-NP*2, to 2.62 Å; correspondingly, the Mulliken charge on Ag_4 becomes as large as −0.65 a.u. All other ions in the polymer follow the displacement of Mg_b, in a sense. At the opposite border, O_b can go very close to Ag_2, due to its decreased ionicity [$q(O_b) = -1.38$ a.u.]. In *E-P*2, the relaxation of Mg_b is less important because two silver atoms are involved, Ag_4 and Ag_6, the latter at about the same height; at equilibrium, the distance of Mg_b from both of them is 2.78 Å.

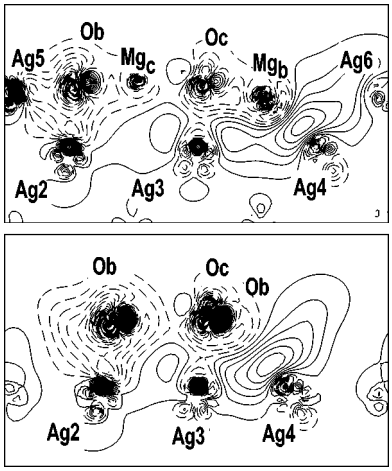

FIG. 4. Density difference maps for the system *E-P*2 (electron density of the interacting system in its equilibrium configuration, minus the superposition of the densities of *P*2 polymer and grooved silver slab calculated independently but at the same geometry). The maps are in a plane normal to the metal surface; their traces in the surface plane are shown in Fig. 1: A—A' (top panel); B—B' (bottom panel). Continuous and dashed lines refer to the positive and negative density difference, respectively. The contour lines are drawn at intervals of $0.01|e|/\text{bohr}^3$.

The analysis of the electronic structure of the systems considered here can provide some clue for interpreting the experimental findings concerning MgO/Ag ultrathin films. Altieri *et al.*[13] extensively investigated the electronic structure of such films at a nominal deposition of $\leqslant 1$ ML, and reported noticeable changes with respect to the unsupported oxide. Using ultraviolet and x-ray photoelectron spectroscopies (UPS and XPS), they observed an appreciable density of states with large oxygen character around and above the Fermi level characterizing the oxide-metal interface. Using XPS and Auger electron spectroscopy they also found a surprisingly high chemical activity of the supported

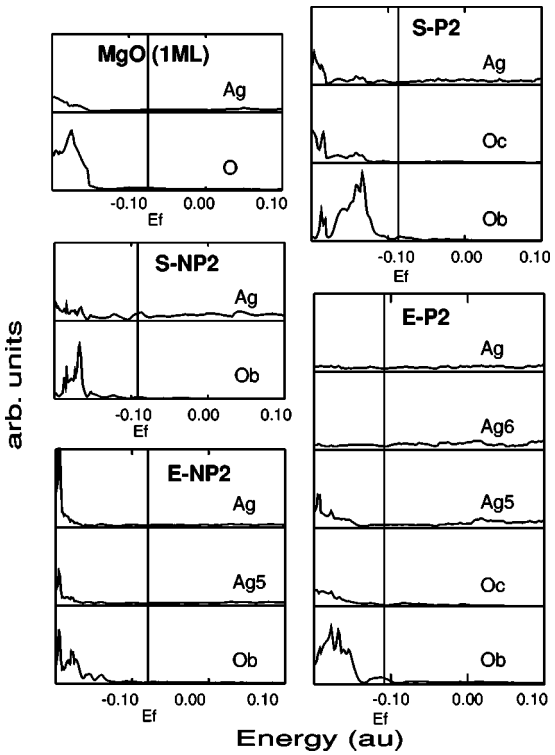

FIG. 5. Atom-projected density of the states (PDOS) of the various model polymers close to the Fermi energy, as indicated. For comparison, the results for the perfect epitaxial monolayer are reported. Ag indicates the average atom in the surface layer. The partition of densities among different atoms is according to a Mulliken population analysis.

film towards H_2O dissociative chemisorption. They argued that this peculiarity was determined by the fact that oxygen derived states moved from the high-binding-energy scale in unsupported MgO to lower energy at the interface. As stated in the Introduction, these kinds of features were not observed in calculations concerning perfect overlayers.[14] The projected densities of states (PDOS) in the vicinity of the Fermi level, reported in Fig. 5, show that the situation can be radically different when polar borders are considered. In both the *S-P*2 and *E-P*2 cases states are present close to the Fermi level, mainly associated with border oxygens, but with a non-negligible participation of surface Ag atoms. These states are indicative of a higher reactivity of bicoordinated O atoms at polar borders.

The enhanced chemical reactivity of the MgO submonolayer can also be related to the presence of unusually high electrostatic fields at the border of the growing film. The role of the electrostatic potential (EP) generated by a surface site in adsorbing, activating and splitting the bonds of polar and nonpolar molecules has been recently discussed.[30] EP maps for the supported and embedded 2-row polymers are collected in Fig. 6 and compared with the MgO (001) surface. Embedded polymers show only a moderate increase of the EP values mostly localized at the Mg border ions. On the contrary the supported polymers (both nonpolar and polar cases) reveal an extraordinary increase of the values of the EP at their border. The hypothesis that border ions are responsible for the observed reactivity of growing oxide overlayers at very low coverages has been recently formulated by Rocca and co-workers.[19,20] The fact that O 1*s* core level BEs are spread out in a range of 2 eV (see Table I) must be attributed to the different EP the anions experience from surrounding ions; due to lower coordination, the shift of border ions is towards lower binding energies. This feature cannot be related to the experimental observation by Altieri *et al.*[9] of the appearance of a second component in the O 1*s* peak observed in aged samples, shifted towards *higher* binding energies by 2.3 eV. That peak must be a consequence of some chemical reaction, most probably with residual water in the vacuum chamber, but these kinds of reactions are not considered in the present work.

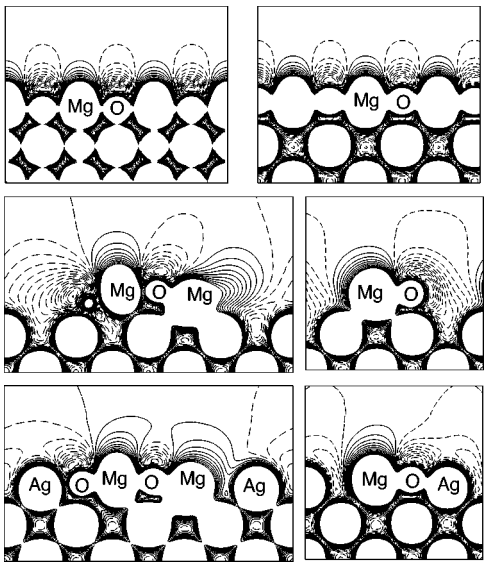

FIG. 6. Electrostatic potential maps. The maps are drawn in a plane normal to the surface and along the ⟨100⟩ oxide symmetry directions. MgO surface (top left panel); MgO monolayer supported at the Ag(001) surface (top right); *S-P*2 model (middle left panel); *S-NP*2 model (middle right panel); *E-P*2 model (bottom left panel); *E-NP*2 model (bottom right panel). Continuous and dashed lines refer to positive and negative values, respectively. The contour lines are drawn at intervals of 0.01 a.u. (1 a.u.=27.21 V).

B. Models for the growth of MgO islands

The present results can be used to discuss the mode of growth of MgO films in the sub-monolayer region. Let us introduce the notion of "energy cost per unit border length" (EB), which measures the difference in energy between an island of oxide at the surface and that of a portion of an infinite ordered overlayer containing the same number of units, divided by the length of the border of the island. EB makes sense if the energetic effects due to the formation of the border are limited to its strict vicinity, which seems to be the case in the present instance, as shown below. For a general shape of the island, EB will correspond to some average value, depending on the orientation of the borders. Here we are interested in comparing EB referring to islands of rectangular shape $\alpha \times \beta$, either *NP*- or *P*-oriented, in order to

TABLE II. Values of e' (energy cost per unit border length) as resulting from the present calculations. For the definition of e' and the identification of the different types of border, see the text. In the case of polymers at grooved slabs, $e'^{*}=e'+fe'_s$, e'_s being the cost of formation of the groove per unit length, and $f=1/2$ or $f=1$ according to whether just one border of the polymer or both are of the "embedded" (E) type.

Type of border		e'(eV/Å)	e'^{*}(eV/Å)	Calculation
(10)	S	0.30		S-$NP1$
(10)	S	0.30		S-$NP2$
(10)	E	0.20	0.27	E-$NP2$
(11)	$1/2(S_O+S_M)$	0.54		S-$P1$
(11)	$1/2(S_O+S_M)$	0.57		S-$P2$
(11)	$1/2(E_O+S_M)$	0.43	0.45	E-$P1_O$
(11)	$1/2(S_O+E_M)$	0.46	0.48	E-$P1_M$
(11)	$1/2(E_O+E_M)$	0.38	0.42	E-$P2$

establish, for a given area, which one is energetically favored. There are two types of *NP* border considered here: $(10)S, (10)E$, the former referring to an island on top of the (001) surface, the latter to a border that leans against a step at the silver surface, of height $a/2$ (a being the silver lattice parameter) and infinite length, and with the same orientation. For P borders the possibilities are four: $(11)S_O, (11)S_M$, $(11)E_O, (11)E_M$; the meaning is the same as for the other orientation, the subscript O or M specifying whether the border is oxygen or magnesium terminated. With reference to the quantity ΔE_{stab} introduced and reported in Table I, an estimate of EB is obtained as follows:

$$e' = \frac{n\Delta E_{stab}}{2l},$$

n being again the number of MgO units per SC, and $2l$ the total length of the border per SC (see Fig. 1). The present calculations allow us to obtain formation energies per unit *wire* length. These are reported in Table II as indicative of the actual e' values, under the assumption previously made about the confinement of energetic effects to the strict vicinity of the border. In the *NP* cases considered, the two borders are equivalent, while for the P ones e' must be considered as an average of two EB's, as indicated. These data lend themselves to some comments. First of all, the cost per unit of length to create a border is far from negligible as it ranges from 0.20 to 0.57 eV/Å; whatever the kind of termination, the edge of an island is much less stable than its inner portion, which can be considered as part of the ideal adsorbed monolayer. Therefore, islands grow so as to reduce the amount of border exposed and realize indeed square or pseudo-square form. In the second place, the data appear consistent among themselves, in the sense that one can obtain reasonable estimates of EB for the different kinds of polar borders [in eV/Å: $\approx$0.57 for $(11)S_O$ and $(11)S_M$, $\approx$0.39 for $(11)E_M$ and $\approx$0.36 for $(11)E_O$] so as to obtain by combination the calculated values of e'. Note incidentally that the difference between the e' estimates obtained from the S-$P1$ and S-$P2$ calculations, may be attributed to the fact that in the former case the attraction between the two polar borders contributes to stabilizing the structure, so the other result seems a better estimate. Third, the e' values for supported polar borders are about twice those for nonpolar ones: for an island growing regularly on a perfect Ag surface, the *NP*-orientation should be by far thermodynamically favored over the other. The difference between the two orientations is considerably reduced in absolute values when "embedded" borders are considered, but the ratio is still quite high ($\approx$1.5). These computational results, however, have to be taken with some caution, due to the limitations of the model adopted, especially as concerns the incomplete geometrical optimization (see Sect. II). Allowing silver atoms at the border to optimize their position might lead to larger energetic advantages for P than *NP* systems, because of the stronger electrostatic field at the former ones. Due to the small difference in energy between the two orientations (a few tenths of eV per silver atom at the border), this could be sufficient to invert the order of stabilities.

Another aspect must be considered that is, the preexistence of defects at the surface. The energy of formation per unit length of a step at the silver surface (e'_s) can be estimated in an analogous way as for e', by comparing the energy of grooved with respect to flat silver slabs. As expected, and in agreement with the data from STM images, silver steps with edges oriented along the $\langle 110\rangle$ direction are favored over the $\langle 100\rangle$ one ($e'_s=0.05$ and 0.07 eV/Å, respectively). These morphological defects are anchoring points for the nucleation of MgO moieties: for geometrical reasons and in the absence of other effects (like metal diffusion) only polar borders should match the $\langle 100\rangle$ stepped edges. Leaning against the metal steps, the nucleation of P-oriented islands is considerably energetically favored over the growth of such an island directly on the terraces, far from pre-existing surface defects (compare $e'=0.43-0.46$ eV/Å and $e'=0.57$ eV/Å for E-$P1$ and S-P islands, respectively, in Table II). The nucleation of P-oriented islands might indeed be kinetically favored because of a larger sticking probability at these sites and therefore they could grow in competition with S-NP islands growing directly on the terraces.

Finally, another scenario is conceivable. Steps and vacancy depressions may not preexist to the MgO deposition (at least not all of them) but are created as the oxide grows. The energy released when MgO monomers form, bind together and stick to the surface, more than compensates for the energy required to displace silver atoms and corrugate the surface. However, the lower cost to create a metal step oriented along the $\langle 110\rangle$ symmetry direction can only partially compensate for the lower stability of polar borders and the resulting e'^{*} for E-P islands is still almost twice as large as the corresponding value for both E-NP and S-NP islands. In any case, the growth of MgO islands embedded in the metal is thermodynamically favored over the growth of supported islands (compare e' values for S-P systems with e'^{*} of E-P cases in Table II). Therefore the oxide might grow by displacing the metal and stabilizing at the positions previously occupied by the metal atoms. However, the activation energy for such a process to happen is not known. The limi-

tations of the present models, first of all the incomplete geometry optimization, does not allow us to make more definite statements about this aspect.

IV. CONCLUSIONS

In this work we have studied the dependence on the morphology of the electronic structure and energetic properties of a submonolayer of MgO deposited at the Ag(001) surface. We have adopted periodic models and *ab initio* DFT calculations employing a gradient corrected functional. In spite of the crudeness of the models adopted, and of the limitations of the calculations (especially as far as geometry optimizations are concerned), some tentative conclusions can be proposed. Notice, however, that all the following considerations are very relevant in the early stages of oxide growth, but they become less important as the film approaches the complete coverage of the metal surface.

(i) *P*-oriented MgO islands, that is with borders along the ⟨110⟩ oxide direction, result in a high dipole moment across them, with a destabilizing effect. Interaction with the metal substrate provides a way to redistribute and to screen the electron charge and enormously contributes to reducing the instability of the polar border (compare ΔE_{ad} and ΔE_{stab} in Table I. Nevertheless, in both the cases of islands supported at the silver surface, or embedded, the role of the metal is not sufficient to stabilize the *P* orientation with respect to the *NP* (nonpolar) one, or to make them of comparable stability. This seems in contrast with the fact that, depending on the experimental conditions, the MgO islands which characterize the morphology of a sub-monolayer are *P* or *NP* oriented. From the literature data it is not clear which are the experimental conditions that should favor the formation of either kind of border.

(ii) The creation of steps or vacancy depressions on the metal with edges oriented along the silver ⟨110⟩ symmetry direction is considerably favored (almost by 25% per unit length) over the ⟨100⟩ oriented edges in agreement with observations. The edges of such steps provide preferential anchoring points for the nucleation and growth of MgO aggregates. In fact the adhesion energy of the MgO aggregates to the metal surface remarkably increases when the oxide is embedded in the metal, Table I. When the steps are preexisting to the nucleation and growth of the oxide, their presence could drive the creation of *P*-oriented MgO islands, the only compatible with ⟨110⟩ oriented edges of the silver steps.

(iii) The nucleation and growth of the oxide embedded in the metal are thermodynamically favored (see Table II): in fact, the adhesion energy between the oxide and the silver substrate more than compensates for the cost to create the metal steps or/and the metal vacancy islands. Nevertheless, which kind of growth can actually occur depends on the kinetic conditions that determine the degree of mobility of the silver atoms. When the conditions of the preparation of the metal substrate, temperature and velocity of deposition of the oxide on the metal surface can favor diffusion of Ag atoms, then the MgO islands may grow by displacing the metal. In this case, the oxide islands would be mainly embedded in the silver upper layers or located near silver steps of the upper terrace.

(iv) The MgO islands, because of their intrinsic defectivity due to the presence of the border, are probably characterized, with respect to the perfect monolayer, by an enhanced chemical activity towards the dissociative chemisorption of small molecules. As suggested by the inspection of EP maps (Fig. 6) and of PDOS data (Fig. 5), this should happen mainly with *P*-oriented borders.

The presented results have to be considered with the awareness of the limitations of the model adopted, especially as concerns the incomplete geometrical optimization (see Sec. II). The relaxation of the silver atoms in response to the interfacial stress and to the charge transfer between the substrate and the oxide island may noticeably affect the stability of the surface structure. In particular, allowing silver atoms at the border to optimize their position might lead to larger energetic advantages for *P* than *NP* systems, because of the stronger electrostatic field at the former ones. Work is in progress to address this aspect.

ACKNOWLEDGMENTS

Useful discussions with Gianfranco Rovida and Sergio Valeri are gratefully acknowledged. Financial support by Istituto Nazionale per la Fisica della Materia (Advanced Research Project ISADORA), and by Italian MURST (COFIN 2003031153, coordinated by G. Pacchioni) is acknowledged.

*Corresponding author; fax: +39-011-670 7855; email address: anna.ferrari@unito.it

[1] S. A. Chambers, Surf. Sci. Rep. **39**, 105 (2000).
[2] G. Renaud, Surf. Sci. Rep. **32**, 1 (1998).
[3] C. T. Campbell, Surf. Sci. Rep. **27**, 1 (1997).
[4] J. Wollschläger, J. Viernow, C. Tegenkamp, D. Erdös, K. M. Schröder, and H. Pfnür, Appl. Surf. Sci. **142**, 129 (1999).
[5] S. Valeri, S. Altieri, A. Di Bona, and C. Giovanardi, Thin Solid Films **400**, 16 (2001).
[6] S. Valeri, S. Altieri, A. Di Bona, P. Luches, C. Giovanardi, and T. S. Moia, Surf. Sci. **507–510**, 311 (2002).
[7] M. Kiguchi, T. Goto, K. Saiki, T. Sasaki, I. Iwasawa, and A. Koma, Surf. Sci. **512**, 97 (2002).
[8] D. Peterka, C. Tegenkamp, K. M. Schröder, W. Ernst, and H. Pfnür, Surf. Sci. **431**, 146 (1999).
[9] S. Altieri, L. H. Tjeng, and G. A. Savatzky, Phys. Rev. B **61**, 24 (2000).
[10] J. Wollschläger, D. Erdös, H. Goldbach, R. Höpken, and K. M. Schröder, Thin Solid Films **400**, 1 (2001).
[11] J. Wollschläger, D. Erdös, and K. M. Schröder, Surf. Sci. **402–404**, 272 (1998).
[12] S. Schintke, S. Messerli, M. Pivetta, F. Patthey, L. Libioulle, M.

Stengel, A. De Vita, and W. D. Schneider, Phys. Rev. Lett. **87**, 276801 (2001).
[13] S. Valeri, S. Altieri, U. del Pennino, A. Di Bona, P. Luches, and A. Rota, Phys. Rev. B **65**, 245410 (2002).
[14] M. Sgroi, C. Pisani, and M. Busso, Thin Solid Films **400**, 64 (2001).
[15] C. Giovanardi, A. Di Bona, T. S. Moia, S. Valeri, C. Pisani, M. Sgroi, and M. Busso, Surf. Sci. Lett. **505**, L209 (2002).
[16] S. Casassa, A. M. Ferrari, M. Busso, and C. Pisani, J. Phys. Chem. B **106**, 12978 (2002).
[17] C. Lamberti, E. Groppo, C. Prestipino, S. Casassa, A. M. Ferrari, and C. Pisani, Phys. Rev. Lett. **91**, 046101 (2003).
[18] P. Luches, S. D'Addato, S. Valeri, E. Groppo, C. Prestipino, C. Lamberti, and F. Boscherini, Phys. Rev. B **69**, 045412 (2004).
[19] L. Savio, E. Celasco, L. Vattuone, and M. Rocca, J. Chem. Phys. **119**, 12053 (2003).
[20] L. Savio, E. Celasco, L. Vattuone, M. Rocca, and P. Senet, Phys. Rev. B **67**, 075420 (2003).
[21] I. Sebastian, T. Bertrams, K. Meinel, and H. Neddermeyer, Faraday Discuss. **114**, 129 (1999).
[22] A. Pojani, F. Finocchi, J. Goniakowski, and C. Noguera, Surf. Sci. **387**, 354 (1997).
[23] C. Noguera, J. Phys.: Condens. Matter **12**, R367 (2002).
[24] A. M. Ferrari, S. Casassa, C. Pisani, S. Altieri, A. Rota, and S. Valeri (unpublished).
[25] V. R. Saunders, R. Dovesi, C. Roetti, R. Orlando, C. M. Zicovich-Wilson, N. M. Harrison, K. Doll, B. Civalleri, I. Bush, P. D'Arco, and M. Llunell, *CRYSTAL 2003 User's Manual*, University of Turin, Torino, 2003.
[26] J. P. Perdew, *Electronic Structure of Solids* (Akademie-Verlag, Berlin, 1991).
[27] S. F. Boys and F. Bernardi, Mol. Phys. **19**, 553 (1970).
[28] E. J. Baerends and O. V. Gritsenko, J. Phys. Chem. A **101**, 5383 (1997).
[29] J. Goniakowski and C. Noguera, Phys. Rev. B **66**, 085417 (2002).
[30] A. D'Ercole, A. M. Ferrari, and C. Pisani, J. Chem. Phys. **115**, 509 (2001).